Dehydroxylation of the Surface of Magnesium Oxide by Temperature Programmed Desorption

Henryk Duński,* Wojciech K. Jóźwiak,† and Henryk Sugier*

*Institute of General Food Chemistry, and †Institute of General and Ecological Chemistry, Technical University of Łódź, ul. Żwirki 36, 90-924 Łódź, Poland

The surface of magnesia acquires adsorptive–catalytic reactivity only after high temperature (HT) dehydration. Temperature-programmed desorption (TPD) of water reveals at least four energetically different forms of adsorbed water. The most significant HT desorption (above 1000 K) exposes low-coordinated (LC) MgO sites which are active sites for hydrogen chemisorption. Water and hydrogen TPD measurements allow the evaluation of the LC site concentration at about 7.5×10^{17} and 7.1×10^{17} site m^{-2}, respectively, which corresponds to about 7% of the total ion surface population. The concentration of the LC sites confirms the much higher heterogeneity of the real MgO surface than that based on simple surface area modelling (about 2.1×10^{17} site m^{-2}). A dehydration mechanism for the energetically heterogeneous surface of magnesia is postulated. © 1994 Academic Press, Inc.

INTRODUCTION

Magnesium oxide is the most important alkaline-earth-metal oxide catalyst and its surface properties have been the subject of extensive investigation (e.g., 1–5). Much attention has been paid to the role of hydroxyl groups in the mechanism of surface hydration and dehydration. These processes are responsible for the creation (or destruction) of surface sites determining the adsorptive–catalytic behaviour of magnesia (6–10). Highly extensive surface dehydroxylation leaves exposed surface defects such as corners, edges, and kinks which have a coordination number (CN) lower than five, the value characterizing the sites on the flat extended surface of MgO. Both theoretical (11, 12) and experimental (9, 11, 13) results strongly indicate that the low-coordinated surface sites of magnesia are involved in the heterolytic splitting of chemical bonds such as H–H, N–H, or C–H (11, 14–18). Magnesia acquires such chemisorptive properties during high temperature (HT) activation in vacuum or inert gas atmosphere, when only a few hydroxyl groups exist on the MgO surface.

Water, which is practically an unavoidable component of the majority of real chemical reactions, plays a decisive role in the physicochemical behaviour of the magnesium oxide surface. A detailed knowledge of the interaction between MgO and H_2O may also be fruitful in modelling the interaction of the magnesia surface with more complex adsorbed molecules possessing an acidic hydrogen atom.

The main objective of this paper has been the determination of the influence of the MgO surface dehydroxylation process on the presence and the reactivity of the low-coordinated sites $Mg_{3C}^{2+} O_{4C}^{2-}$ and $Mg_{4C}^{2+} O_{3C}^{2-}$, which are the corners of the MgO crystal (100) face. The temperature-programmed desorption of hydrogen (TPD_{H2}) was used as a discriminative method to detect the low coordinated sites on the surface of MgO. This sensitive method, originally adopted by Ito et al. (15, 19), is a good complementary tool to IR and photoluminescence measurements of the surface hydration and dehydration processes on magnesia (6, 8, 10).

EXPERIMENTAL

Magnesium oxide (BDH Chemicals Ltd, high purity grade) with surface area 75.5 m^2 g^{-1} (BET method, liquid N_2) and hydrogen (Technische-Gase-Leipzig, specially pure grade) were used. The sample of MgO (0.002–0.1 g), placed in a quartz vessel with diameter 30 mm, was purified by vacuum treatment (bellow 1.3×10^{-4} Pa) at high temperature (usually at 1250 K) during 2 h. After being cooled to ambient temperature the MgO surface was heavily hydrated by prolonged contact with water vapour (p_{H2O} = 1250 Pa). Water was previously degassed by the freeze–thaw method. After such treatment samples were activated (1 h) in the temperature range 650–1250 K in vacuo. The conditions of the above procedure were adopted to ensure that the MgO surface was covered only with hydroxyl groups. A blank TPD run of the magnesium oxide previously degassed at 1250 K reveals only very small desorption effects above 1150 K, attributed to residual gas readsorption from the background vacuum. Partial hydration of the MgO surface was accomplished by expo-
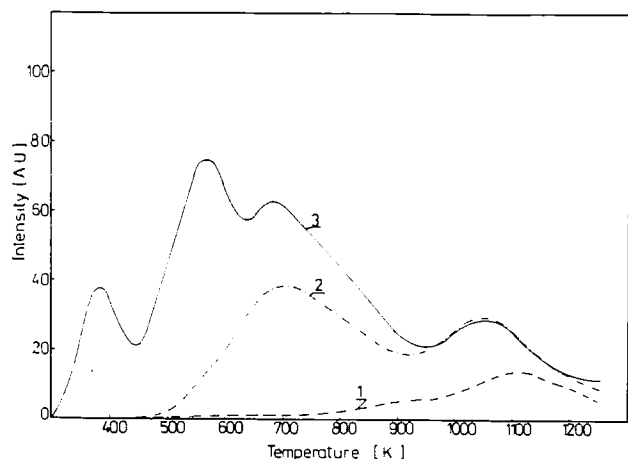
FIG. 1. TPD$_{H2O}$ profiles for MgO after hydration at ambient temperature. Curves 1–3 refer to coverage θ: 0.04, 0.17 and 0.34, respectively.

sure at 293 K to a known amount of water vapour with initial pressure $p/p_0 = 1.6 \times 10^{-2}$.

Hydrogen adsorption at ambient temperature (usually $p_{H2} = 106$ Pa for 2 h) was followed by cooling to 80 K. TPD measurements were carried out in the vacuum dynamic system described earlier (20). The linear temperature increase was 20 K min^{-1} for TPD$_{H2O}$ and 10 K min^{-1} for TPD$_{H2}$ measurements and was controlled by a microprocessor system. An ion gauge was used as a detector of hydrogen or water pressure. In the case of TPD$_{H2}$ measurements, a liquid nitrogen trap was usually used to eliminate gases such as H$_2$O or CO$_2$ that were either present in the background gas atmosphere or desorbing from the MgO surface. An occasionally adopted additional HT calcination of MgO in oxygen atmosphere did not result in any noticeable change of our TPD$_{H2O}$ or TPD$_{H2}$ profiles. Thus, the level of carbonaceous impurities was negligibly small. Quantitative evaluation of TPD results was based on integration of the area under the TPD profile after calibration. The TPD profiles were recorded after a previous evacuation at the starting temperature.

The reproducibility of the TPD profiles was ca ±5% on repeated runs. The actual accuracy of the hydrogen desorption evaluation was ±10% and for the water desorption it was ±20% in the worst case.

RESULTS

Water Thermodesorption

The TPD profiles of water strongly depend on the degree of magnesia surface hydration; this relationship is shown in Fig. 1. In order to achieve surface equilibrium prior to the TPD run the MgO sample was preheated to 450 K during 0.5 h in a controlled atmosphere of water

vapour and then was cooled back to the ambient temperature. The low hydroxyl group coverage $\theta = 0.04$ is represented by TPD$_{H2O}$ profile 1 in Fig. 1, showing that water desorption starts above 600 K and then steadily increases its rate to reach a maximum at T_{max} about 1110 K. The θ values were calculated assuming dissociative adsorption of water which takes place on the dominant (100) crystal face of MgO (1, 2). Thus, the monolayer hydroxyl group coverage ($\theta = 1$) corresponds to an OH group attached to each surface Mg^{2+} cation and an H atom attached to each surface O^{2-} lattice anion (thereby forming a second OH group), yelding total OH group density of 2.2×10^{19} OH group m^{-2} (6). The much more complex TPD$_{H2O}$ profile 3 in Fig. 1 is observed for $\theta = 0.34$ with several succeeding maxima at about 370, 570, 680, and 1050 K, respectively. The first peak ($T_{max} = 370$ K) represents the water molecules physically adsorbed via hydrogen bonding with already existing hydroxyl groups (8), whereas the remaining peaks originate from the process of dehydroxylation of the magnesia surface. The intermediate character of TPD$_{H2O}$ profile 2 in Fig. 1 refers to the hydroxyl group surface coverage $\theta = 0.17$. After the ambient temperature hydration the residual water vapour pressures were below 0.1 Pa for $\theta = 0.04$ and $\theta = 0.17$ but about 1.3 Pa for $\theta = 0.34$.

Water is readily absorbed at ambient temperature on thermally activated MgO, even under a very low pressure of water vapour (e.g., 6.7×10^{-2} Pa or $p/p_0 = 2.9 \times 10^{-5}$). The influence of the adsorption time on the early stage of the surface rehydroxylation process is shown in Fig. 2. Increase of the adsorption time from 3 to 10 min resulted in an OH coverage enhancement from $\theta = 2.4 \times 10^{-3}$ to $\theta = 7.8 \times 10^{-3}$. Although the desorption of water starts above 600 K, the main amount of water is desorbed above 1000 K. Regardless of the possible readsorption effects
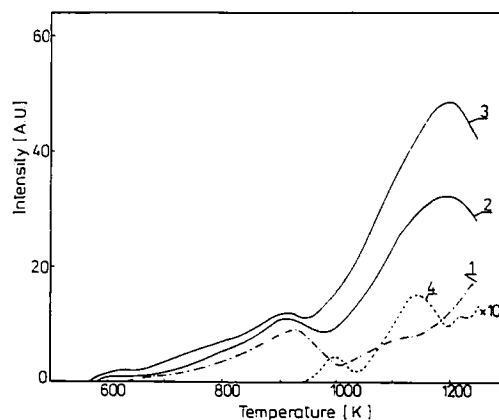

FIG. 2. TPD$_{H2O}$ profiles after MgO exposure at ambient temperature to 6.7×10^{-2} Pa of H$_2$O ($p/p_0 = 2.9 \times 10^{-10}$) at ambient temperature. Curves 1-3 refer to time: 3, 6, and 10 min, respectively; 4: the same as 3 but only the noncondensable gases in the liquid N$_2$ trap were recorded.
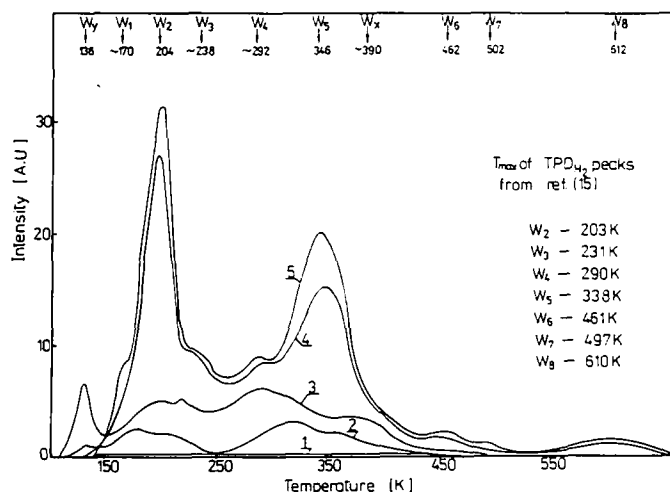
FIG. 3. TPD$_{H2}$ profiles as a function of the MgO pretreatment temperature. Curves 1–5 refer to 650, 800, 950, 1100, and 1250 K, respectively.

taking place during a TPD$_{H2O}$ run, the major part of the released water originates from the most tightly bound hydroxyl groups. Desorption of this strongly held water is accompanied by comparatively small (below 4%) desorption of gases (profile 4 in Fig. 2) which are noncondensable in the liquid nitrogen trap (probably H$_2$ and O$_2$ or both). The emission from cell walls was negligibly small. High temperature hydrogen and oxygen desorption effects accompanying the Mg(OH)$_2$ dehydration have been observed by Martens et al. (21) and Derouane et al. (22). They postulated the formation of cationic vacancies in the course of magnesia dehydration.

Hydrogen Thermodesorption

The influence of the magnesia activation temperature on the hydrogen thermodesorption profiles is shown in Fig. 3. Very similar pretreatment and adsorption conditions and the same TPD$_{H2}$ peak notation as those reported by Ito et al. (15, 19) were adopted in order to verify the TPD$_{H2}$ procedure as a discriminative method for the detection of low-coordinated sites on the MgO surface. The TPD$_{H2}$ profiles shown in Fig. 3 indicate that the surface of magnesia reveals progressive hydrogen chemisorption reactivity effects starting at an activation temperature above 650 K and reaching maximum effect after pretreatment of MgO at 1250 K. A good mutual qualitative accordance of the results presented in Fig. 3 with those reported by Ito et al. (19) was confirmed. The only substantial difference refers to a relatively smaller total amount of desorbed hydrogen (calculated per square meter), about 37% of the value reported by Ito et al. (19). The probable reason for the difference was the higher surface area of their MgO sample (ca. 200 m^2 g^{-1}). In

addition, the intermediate TPD peaks denoted as W_x and W_y were found after the activation of magnesia at 800 and 950 K.

Assuming that the particular TPD$_{H2}$ peaks in Fig. 3 represent hydrogen desorption from the respective low-coordinated sites of the MgO surface, one can assign peaks W_2 and W_3 to Mg$_{3C}^{2-}$ O$_{4C}^{2-}$, W_4 and W_5 to Mg$_{4C}^{2+}$ O$_{3C}^{2-}$, and W_6–W_8 to Mg$_{3C}^{2+}$ O$_{3C}^{2-}$ surface ion pair sites (15, 19), and denote these types of sites as A, B, and C, respectively. The assignment of a few (two or three) hydrogen desorption peaks to one low-coordinated ion pair site reflects the influence of the chemically different environment surrounding the respective surface site of magnesia. The detailed considerations referring to W_2–W_8 peaks were previously given by Ito et al. (19). The quantitative evaluation of the LC site concentration (A, B, C) on the magnesia surface is shown in Fig. 4 as a function of the activation temperature. Starting from 650 K, the magnesia surface steadily develops its chemisorption activity reaching the maximum site concentration after activation at 1250 K.

Hydrogen chemisorption on the MgO surface is conditioned by the exposure of the LC sites as a result of surface dehydroxylation (see the inset in Fig. 4 (8)). The chemisorption of hydrogen starts when the hydroxyl group coverage θ falls below 0.25 and is a maximum when there are practically no hydroxyl groups on the MgO surface.

The influence of the activation time at 1200 K on the concentration of the respective A, B, and C type sites is shown in Table 1. A and B sites are dominant and their concentration is nearly the same and approximately equal
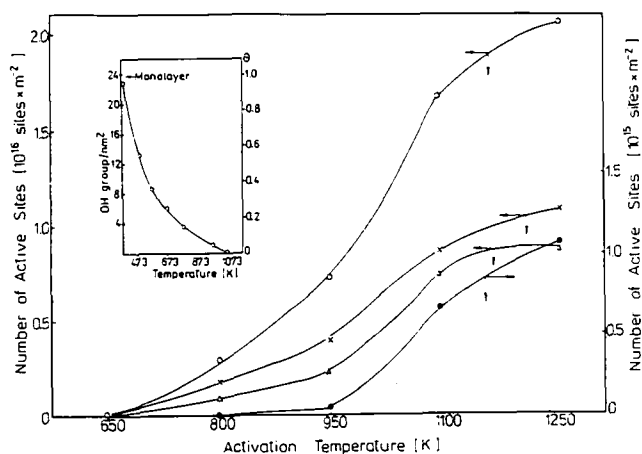

FIG. 4. The concentration of the low-coordinated (LC) sites on MgO surface as a function of the activation temperature: (O) total concentration (A + B + C); (x) type A; (Δ) type B; (●) type C. Inset: residual OH groups on the surface of MgO after outgassing (30 min) at increasing temperatures. The magnesium oxide was previously rehydrated at 298 K for 40 min (8).

TABLE 1

The Low-Coordinated Site Concentration as a Function of the Activation Time of MgO at 1200 K

Time (h)	Site concentration			
	A	B	C	Total
1	0.86×10^{16}	1.0×10^{16}	1.1×10^{15}	2.0×10^{16}
2	1.10×10^{16}	1.0×10^{16}	1.2×10^{15}	2.2×10^{16}
5	1.15×10^{16}	1.0×10^{16}	1.3×10^{15}	2.3×10^{16}

to 1.0×10^{16} site m^{-2}. The concentration of type C sites is one order of magnitude lower (about 1.2×10^{15} site m^{-2}) and so these sites will not be further considered. Thus, the total concentration of the LC sites is in the range $(2.0–2.3) \times 10^{16}$ site m^{-2} depending on the activation time (Table 1). One can note that the population of B sites is constant whereas A sites become more numerous (about 30%) when the activation time changes from 1 to 5 h.

On the temperature-activated surface of magnesium oxide, besides reversibly bonded hydrogen (Fig. 3), we also observed irreversibly bonded hydrogen finally desorbing as water molecules above 800 K. For example, in favourable conditions (450 K, $p_{H2} = 1.6$ kPa, 20 h), the amount of desorbed water was about 2.5×10^{15} H_2O molecule m^{-2}.

It is fairly obvious that at least a part of the MgO surface adsorption sites (the low-coordinated sites) are common for adsorption of both water and hydrogen molecules (see Fig. 4). The influence of preadsorbed water on hydrogen TPD profiles is shown in Fig. 5. The water preadsorbed ($\theta = 0.031$) at ambient temperature and equilibrated at 450 K blocks about 41% of sites A and about 50% of sites B. The adsorption of the same amount of water only at
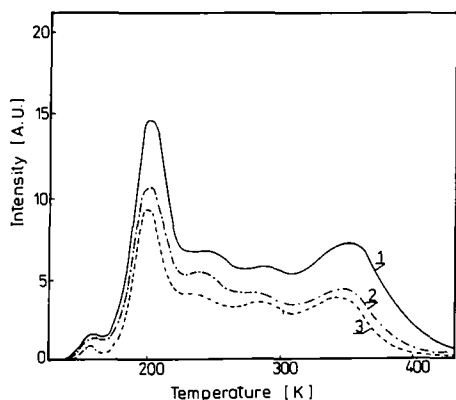

FIG. 5. TPD_{H2} profiles for MgO after water preadsorption: (1) unhydrated sample, (2) 1 h H_2O adsorption at 293 K ($\theta = 0.031$), (3) the same as 2 plus 0.5 h at 450 K and cooling at 293 K.

ambient temperature leads to a somewhat smaller blocking effect.

DISCUSSION

The developing complexity of the water thermodesorption profiles as a function of the increasing degree of surface hydroxylation directly points to the MgO surface heterogeneity as being primarily responsible for the different thermal stability of the surface hydroxyl groups existing on magnesia (Fig. 1). In general, for low degrees of hydroxylation (θ lower than 0.01) essentially only high temperature desorption (above 1000 K) is observed (Fig. 2). The additional low and medium temperature desorption of water is a result of the high degree of surface hydroxylation.

The hydroxyl group heterogeneity on magnesia surface is not unexpected if the following are taken into account:

(1) the structural differences between OH groups fixed to Mg^{2+} and O^{2-} ions;

(2) the different environment of the OH group bonded to the fivefold coordinated size on the (100) face in comparison to the four- and three fold coordinated sites occupying the edges and corners of MgO crystallites, respectively;

(3) the involvement of the OH group hydrogen bonding with the vicinal hydroxyl groups.

The magnesia surface acquires its maximum chemisorptive–catalytic reactivity during high temperature (above 1000 K) vacuum or inert gas treatment (11, 14–18, 23, 24). The hydrogen chemisorption reactivity of magnesia is illustrated in Figs. 3–5. The course of the water adsorption–desorption process conditioning the presence of the exposed LC sites on the magnesia surface plays a crucial role.

In relation to the above statements let us evaluate more precisely the population of the LC sites on the magnesia surface. The specific surface area of 75.5 m^2 g^{-1} corresponds to the average dimension of the cubic crystals being about 23 nm. This value results in about 2.6×10^{15} ion crystal corners (sites A and B) and about 2.1×10^{17} edge sites (Mg_{4C}^{2+} O_{4C}^{2-}) per square meter of MgO. The much higher experimental value of about 2.2×10^{16} corner site m^{-2} (Fig. 4) strongly suggests the much more defective real texture of MgO surface, comprising terraces, edges, steps, and kinks (9, 25). Assuming a uniform distribution of corner sites on the MgO surface, one can estimate the concentration of the edge sites resulting in about 6.9×10^{17} site m^{-2}. The total concentration of all low-coordinated sites (coordinated number CN < 5), comprising besides the edge and corner sites (A, B) also the so-called separated ions (Mg_{3C}^{2+} O_{5C}^{2-} or Mg_{5C}^{2+} O_{3C}^{2-}), would be about 7.1×10^{17} LC site m^{-2}. These separated ions can be

responsible for the homolytic dissociation of hydrogen, resulting in hydroxyl group formation (26). Our results on hydrogen adsorption confirm the possible existence of sites of this type. Recently, Knözinger et al. reported that irreversible homolytic hydrogen adsorption may take place on neighboring three-coordinated O_{3C}^- · radical anions in (111) microplanes (27). The calculated value of the LC population is in good accordance with the maximum high temperature desorption of water (HT peak in Fig. 1) being about 1.5×10^{18} OH group m^{-2}. Taking into account that two hydroxyl groups are located on one LC site, the mutual agreement between the calculated and experimental values strongly supports the idea that the most tightly bound hydroxyl groups originate from the low-coordinated sites of the magnesia surface. This conclusion is in accordance with the hydrogen thermodesorption results (Fig. 4), which indicate that the hydroxyl groups, strongly bound to the LC sites, condense in the last stage of MgO dehydration. This concept, reported by us earlier (28), is identical to that formulated on the basis of IR measurements by Coluccia et al. (8) and photoluminescence spectroscopy (10).

The residence time of the adsorbed water molecule (t) on the adsorbent surface depends upon the enthalpy of adsorption (ΔH) according to the equation

$$t = t_0 \exp(\Delta H/RT), \qquad [1]$$

where t_0 is the time of vibration of the adsorbed molecule, which is about 10^{-13} s (29). Taking into account the molecular adsorption of water on MgO surface at ambient temperature and assuming the ΔH values 1, 62, and 86 kJ mol^{-1} for the particular flat, edge, and corner MgO sites (30), one can obtain the adsorbate residence times as 10^{-13}, 10^{-2}, and 10^2 s, respectively. This rough estimate clearly points to the LC sites (edges and corners) as the destination anchorage sites for water molecules, where the dissociative chemisorption occurs. The water molecules initially adsorbed on flat surface sites, contributing to about 93% of the entire surface ion population, readily return to the gas phase without dissociation. Only the exposed LC sites with coordination number (CN) of 4 (or 3) undergo the hydroxylation process in the early stages of MgO hydration (9, 10). Theoretical (30) and experimental (9, 17) investigations have shown that the LC sites of MgO are the favorable sites for both molecular and dissociative chemisorption of water. On the other hand, the magnesia surface without the LC sites is very resistant towards hydroxylation (9, 31). Generally, the adsorption of water on MgO at the early stage of hydration does not distinguish between the energetically strong corner (CN = 3) and edge (CN = 4) sites. The preadsorbed water ($\theta = 0.031$) blocks rather uniformly both type A and type B corner sites (about 45%) and edge sites (below 43%).

This latter value results from the calculated material balance. A weak tendency to preferable blocking of type B rather than type A sites was observed after the pretreatment of MgO at ambient temperature (profile 2 in Fig. 5).

However, this simple model of the early stage of MgO hydration does not explain the observed medium temperature desorption effects when the hydroxyl group coverage ($\theta < 0.01$) is lower than the total concentration of the LC (edge and corner) magnesia sites (Fig. 2). One can even suppose that the possible readsorption effects taking place during the TPD_{H2O} run diminish the experimental evidence of more weakly bonded OH group desorption. Thus, we are forced to assume that the already existing LC–OH site facilitates the second step of the hydroxylation process in the direct vicinity for the next adsorbed water molecule. This simply means that the next to edge line sites would be more favourable for water adsorption than those lactated far away on flat magnesia surfaces. Two reasons may favour such a situation. First, in spite of the edge site being already occupied by one OH group, the local unsaturation of the near edge site is higher than that characteristic of the typical central location site. Second, the already existing edge (or corner) OH group may be involved in hydrogen bonding with the attacking water molecule, delivering the extra stabilization component of the $MgO-H_2O$ interaction. The already formed or residual hydroxyl groups would play a very important role as the nucleation centres in the near edge regions of magnesia surface. This fast and irreversible hydroxylation would result in 15–25% monolayer coverage (profiles 1 and 2 in Fig. 1).

The remaining exposed flat MgO surface appears much more resistant toward hydroxylation. High residual water vapour pressure (profile 3 in Fig. 1) was observed although the achieved coverage corresponded merely to 0.31 hydroxyl group monolayer. Besides, the low temperature desorption peak (T_{max} about 370 K) clearly shows the presence of molecularly bonded water on the MgO surface (about 3% of a monolayer). The activation energy of desorption for the molecular adsorbed water (via strong hydrogen bonding) on existing hydroxyl groups has been estimated as 94 kJ mol^{-1} (29, 32). Anderson et al. (6) found that the heat of desorption of the physisorbed water is about 83 kJ mol^{-1}. These relatively high values suggest that the water molecule is located (via hydrogen bonding) on the already hydroxylated LC magnesia sites (8). The ratio of the amount of physically adsorbed water ($\theta = 0.031$) to the total concentration of the LC sites ($\theta = 0.07$) is about 0.42. This value suggests that the H_2O molecule is adsorbed on two hydroxyl groups through hydrogen bonding (33).

The possible reason for this rather slow and activated process of the advanced hydroxylation stage (8, 30) may result from the unavoidable rearrangement of the random

distribution of the hydroxyl pairs into the uniform well-ordered monolayer of hydroxyl groups. This two-dimensional OH group surface reconstruction requires either the splitting of some existing Mg–OH bonds or at least the considerable mobility of hydrogen atoms (protons) over the MgO surface and these processes depend strongly on time, temperature, and water vapour pressure (6, 8, 33). The increase of the water vapour pressure promotes the accomplishment of the OH monolayer formation by delivering the second layer of the weakly bonded H_2O molecules in which proton migration is probably an effective process.

The dehydration process described above is in good agreement with IR investigations (6, 8, 33, 34). However, Gu and Brenner (35) rather surprisingly claim that a hydroxyl group monolayer exists on the MgO surface even after dehydration at 823 K. Our results do not confirm this conclusion.

Assuming the validity of the model of the $MgO–H_2O$ interaction presented above one can attribute the following TPD_{H2O} peaks (profile 3 in Fig. 1) to the subsequent stages of magnesia dehydration:

T_{max} about 370 K—desorption of water molecules weakly bonded (via hydrogen bonding) with hydroxylated MgO surface;

T_{max} about 570 K—desorption of water molecules as a result of hydroxyl group pair condensation on the flat surface of MgO;

T_{max} about 700 K—desorption of more strongly bound water from the vicinity of the LC MgO sites and the removal of the more isolated remaining hydroxyl groups on flat surface;

T_{max} about 1150 K—desorption of water from the LC MgO sites.

Thermal dehydration is not a simple reversal of ambient temperature hydration. This is especially true for the last stage of dehydration in comparison with the very first stage of hydration. Both processes appear to be essential conditioning for the chemisorptive—catalytic behaviour of MgO. For instance, the LC corner sites dissociate H–H and C–H bonds (11, 15), whereas when bonded with single OH groups they are active in the $H_2–D_2$ exchange reaction (35, 36) and in the $O_2–OH$ exchange for CaO (37). Echterhoff et al. (34) have found that already in the first seconds of MgO hydration (p_{H2O} = 133 Pa) only bulk hydroxyl groups and surface complexes incorporating physisorbed water are formed. Bulk hydroxyl group formation was not confirmed by Coluccia et al. (8). Free and isolated groups do not appear in IR spectra in the early stage of MgO hydration (8, 32, 33). In contrast, during the very last stage of high temperature dehydration the isolated OH groups (fixed to the most unsaturated LC sites (8, 27)) dominate. The dehydration model of the residual hydroxyl
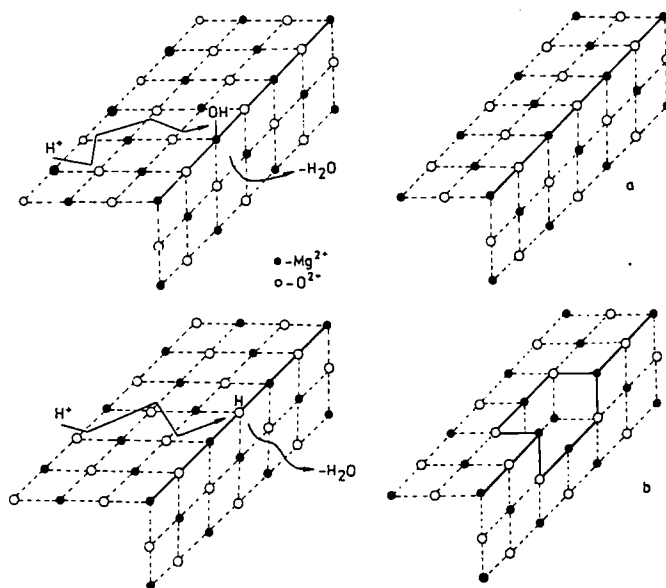

FIG. 6. Dehydration model of the residual hydroxyl groups on MgO surface.

groups on magnesia surface is presented in Fig. 6. Dehydroxylation involving the mobile surface proton and the isolated OH group located on Mg^{2+} ion does not increase the concentration of LC sites (Fig. 6a). If the lattice O^{2-} constitutes the hydroxyl group, the dehydroxylation may result in the additional type A corner site formation (Table 1) according to the scheme in Fig. 6b. This concept was originally proposed by Peri (38) for alumina surfaces and was postulated for MgO by Coluccia et al. (8). The release of hydrogen and oxygen during high temperature dehydration seems to confirm that the surface reconstruction takes place.

ACKNOWLEDGMENT

REFERENCES

1. Boudart, M., Delbouiille, A., Derouane, E. G., Indovina, V., and Walters, A. B., *J. Am. Chem. Soc.* **94**, 6622 (1972).
2. Zecchina, A., Lofthouse, M. G., and Stone, F. S., *J. Chem. Soc. Faraday Trans.* **71**, 1476 (1975).
3. Hattori, H., Shimazu, K., Yoshii N. and Tanabe, K., *Bull. Chem. Soc. Jpn.* **49**, 969 (1976).
4. Segall, R. L., Smart, R. St. C., and Turner, P. S., *J. Chem. Soc. Faraday Trans. 1* **74**, 2907 (1978).
5. Coluccia, S., Tench, A. J., and Segall, R. L., *J. Chem. Soc. Faraday Trans. 1* **75**, 1769 (1979).
6. Anderson, P. J., Horlock, R. F., and Oliver, J. F., *Trans. Faraday Soc.* **61**, 2754 (1965), and references therein.
7. Faure, M., Fraissard, J., and Imelik, B., *Bull. Soc. Chim.*, 2283 (1967), and references therein.

8. Coluccia, S., Lavagnino, S., and Marchese, L., *Mater. Chem. Phys.* **18**, 445 (1988), and references therein.

9. Jones, C. F., Reeve, R. A., Rigg, R., Segall, R. L., Smart, R. St. C., and Turner, P. S., *J. Chem. Soc. Faraday Trans. 1* **80**, 2609 (1984).

10. Duley, W., *J. Chem. Soc. Faraday Trans. 1* **80**, 1173 (1984).

11. Ito, T., Tashiro, T., Kawasaki, M., Watanabe, T., Toi, K. and Kobayashi, H., *J. Phys. Chem.* **95**, 4476 (1991).

12. Kobayashi, H., Yamaguchi, M., and Ito, T., *J. Phys. Chem.* **94**, 7206 (1990).

13. Colbourn, E. A., and Mackrodt, W. C., *Surf. Sci.* **117**, 571 (1982).

14. Coluccia, S., Boccuzzi, F., Ghiotti, G., and Morterra, C., *J. Chem. Soc. Faraday Trans. 1* **78**, 2111 (1982).

15. Ito, T., Kuramoto, M., Yoshioka, M., and Tokuda, T., *J. Phys. Chem.* **87**, 4411 (1983).

16. Coluccia, S., and Tench, A. J., *in* "Proceedings, 7th International Congress on Catalysts, Tokyo, 1980" (T. Seiyama and K. Tanobe, Eds.), p. 1154. Kodansha/Elsevier, Tokyo/Amsterdam, 1981.

17. Garrone, E., and Stone, F. S., *in* "Proceedings, 8th International Congress on Catalysts, Berlin, 1984," Vol. 3, p. 441. Verlag Chemie, Weinheim, 1984.

18. Echterhoff, R., and Knözinger, E., *Surf. Sci.* **230**, 237 (1990).

19. Ito, T., Murakami, T., and Tokuda, T., *J. Chem. Soc. Faraday Trans. 1* **79**, 913 (1983).

20. Duński, H., and Sugier, H., *Phys. Status Solidi A* **116**, K165 (1989).

21. Martens, R., Gentsch, H., and Freund, F., *J. Catal.* **44**, 366 (1976).

22. Derouane, E. G., Fripiat, J. C., and André, J. M., *Chem. Phys. Lett.* **28**, 445 (1974).

23. Ito, T., and Lunsford, J. H., *Nature (London)* **314**, 721 (1985).

24. Zecchina, A., Coluccia, S., and Morterra, C., *Appl. Spectrosc. Rev.*, **21**, 259 (1985).

25. Coluccia, S., Barton, A., and Tench, A. J., *J. Chem. Soc. Faraday Trans. 1* **77**, 2203 (1981).

26. Ito, T., Kawanami, A., Toi, K., Shirakawa, T., and Tokuda, T., *J. Phys. Chem.* **92**, 3910 (1988).

27. Knözinger, E., Jacob, K. H., and Hofmann, P., *J. Chem. Soc. Faraday Trans. 1* **89**, 1101 (1993).

28. Duński, H., and Sugier, H., *React. Kinet. Catal. Lett.* **37**(2), 481 (1988).

29. de Boer, J. H., "The Dynamical Character of Adsorption," Chap. 3. Oxford Univ. Press, Oxford, 1953.

30. Zanpeisov, N. U., Pelmenchikov, A. G., and Zidomirov, G. M., *Kinet. Katal.* **32**(4), 970 (1991).

31. Peng, X. D., and Barteau, M. A., *Surf. Sci.* **233**, 283 (1990).

32. Cvetanovic, R. J., and Amenomiya, Y., *Catal. Rev.* **6**, 21 (1972).

33. Kuroda, Y., Yasugi, E., Aoi, H., Miura, K., and Morimoto, T., *J. Chem. Soc. Faraday Trans. 1* **84**, 2421 (1988).

34. Echterhoff, R., Hoffman, P., and Knözinger, E., *in* "Proceedings, 9th International Congress on Catalysis, Calgary, 1988" (M. Ternan and M. J. Phillips, Eds.), Vol. 3, p. 1418. Chem. Inst. Canada, Ottawa, 1988.

35. Gu, Y., and Brenner, A., *J. Catal.* **136**, 222 (1992).

36. Ito, T., Tominaga, N., Tashiro, T., Toi, K., Ikemoto, I., and Kobayashi, H., *Bull. Chem. Soc. Jpn.* **63**, 3016 (1990).

37. Cunningham, J., and Healy, C. P., *J. Chem. Soc. Faraday Trans. 1* **83**, 2973 (1987).

38. Peri, J. B., *J. Phys. Chem.*, **69**, 220 (1965).